

Time-resolved Spectroscopy of Glass Ablation during Micro-via Processing using 248 nm Excimer Laser for Semiconductor Interposer Packaging

Yasufumi Kawasuji^{*1}, Yasuhiro Adachi¹, Kazuhiko Moro¹, Kouji Kakizaki¹, and Masakazu Washio²

¹Gigaphoton Inc. 400 Yokokura-shinden, Oyama-shi, Tochigi 323-8558, Japan

²Waseda University 3-4-1 Okubo, Shinjuku-ku, Tokyo 169-8558 Japan

^{*}Corresponding author's e-mail: yasufumi_kawasuji@gigaphoton.com

A glass interposer with micro-vias is promising for next-generation semiconductor packaging for post-5G high performance computing. Glass is the most promising material due to its electrical and mechanical characteristics; however, it is difficult to fabricate micro-vias in glass due to its high brittleness. The fabrication speed should also be improved to realize the commercialization of glass interposers. We have researched improvements in the production of micro-vias in glass, and optical systems with glass micro-vias. Processing glass material a 248 nm excimer laser was found to produce micro-vias ($<15\ \mu\text{m}$ diameter) with very high aspect ratios (>33) and very high quality (no microcracks). Furthermore, long laser pulse widths (74 ns time-integrated square (TIS)) resulted in a higher drilling rate than short pulse widths (32 ns TIS). Herein, we report the results of spectroscopy measurements for the ablation of glass using a 248 nm excimer laser, together with the results of time-resolved spectroscopy. We also report the pulse width dependence of the time-resolved spectroscopy results for short and long laser pulses to determine the reason for the high drilling rate for a long pulse width. The measurement results indicated that the wavelengths of light emitted during ablation were mainly 280, 394, 422 nm. This emission began 30 ns after laser irradiation was started. We consider that absorption increases after laser irradiation, and that it takes approximately 30 ns for the laser energy to be absorbed and the ablation threshold to be reached. The time at which ablation occurred was almost constant, regardless of the excimer laser pulse width, even though the intensity of the long laser pulses was lower than that of the short pulses. The results indicate that a larger amount of laser energy is wasted during short-pulse laser drilling until ablation begins, so that a higher drilling rate is achieved with long pulses.

DOI: 10.2961/jlmn.2022.03.2001

Keywords: glass, interposer, micro-via, excimer laser, ablation, spectroscopy

1. Introduction

Semiconductor integration has continued to improve over the past 50 years in accordance with Moore's Law. However, it has almost reached the resolution limit with respect to miniaturization. One alternative solution is multi-die packaging using either organic films or single-crystal silicon wafers as substrates. However, single-crystal silicon wafers have a very high manufacturing cost, and miniaturization of organic films has almost reached its limit due to their shape distortion.

Non-alkali glass is expected to be good alternative substrate material for multi-die packaging due to its low production cost and its high shape stability. Furthermore, glass has the advantage of a very low electrical loss for high-frequency signal applications such as 5G and post-5G telecommunications. The plate of the substrate for multi-die packaging is called an interposer and it will be referred to as such. However, it is difficult to fabricate micro-vias in glass due to its high brittleness [1][2][3].

We have established that high-quality, high-aspect processing can be achieved by ablating non-alkali glass with

an excimer laser at a wavelength of 248 nm [4]. The excimer laser can easily generate a large laser power of several hundred watts, which makes it is possible to drill many holes at the same time, whereby the machining cost can be significantly reduced.

We conducted research to further reduce drilling costs for a glass interposer substrate and determined that increasing the laser pulse width using an optical pulse stretcher (OPS) can increase the drilling rate.

Here, we report the results of time-resolved spectroscopy for the ablation of non-alkali glass as the substrate of a glass interposer using a 248 nm wavelength excimer laser. The differences between the results for long laser pulses (74 ns time-integrated square (TIS)) and short laser pulses (32 ns TIS) are also reported. We also propose a mechanism to explain the high drilling rate achieved with long laser pulses.

2. Experimental Setup

Figure 1 shows a schematic diagram of the test setup used for micro-drilling glass substrates with the excimer laser. The experimental parameters are shown in Table 2. A Gigaphoton GT600K excimer laser was used for the drilling process. The main laser light source parameters are given in Table 1. The TIS range for the laser output pulse is 32–74 ns. All experiments were performed in ambient air and under the same conditions expected in practical applications. The laser fluence was adjusted using an optical attenuator. The beam shape on the material surface was formed using an aperture and a lens.

Table 1 Main output parameters for Gigaphoton GT600K excimer laser light source.

Wavelength [nm]	248
Pulse energy [mJ/pulse]	100
Repetition rate [Hz]	10–6000
Output laser power [W]	600
Pulse width TIS [ns]	32, 74

Aperture diameter [mm]	0.5 (round shape)
Focal length of lens [mm]	54 (@248 nm wavelength)
Sample position [mm]	The sample surface plane is conjugated with the aperture plane. Distance between aperture and lens: 1700

Table 2 Experimental parameters.

The TIS value is given by

$$TIS = \frac{[\int I(t)dt]^2}{\int I(t)^2 dt}$$

where $I(t)$ is the intensity.

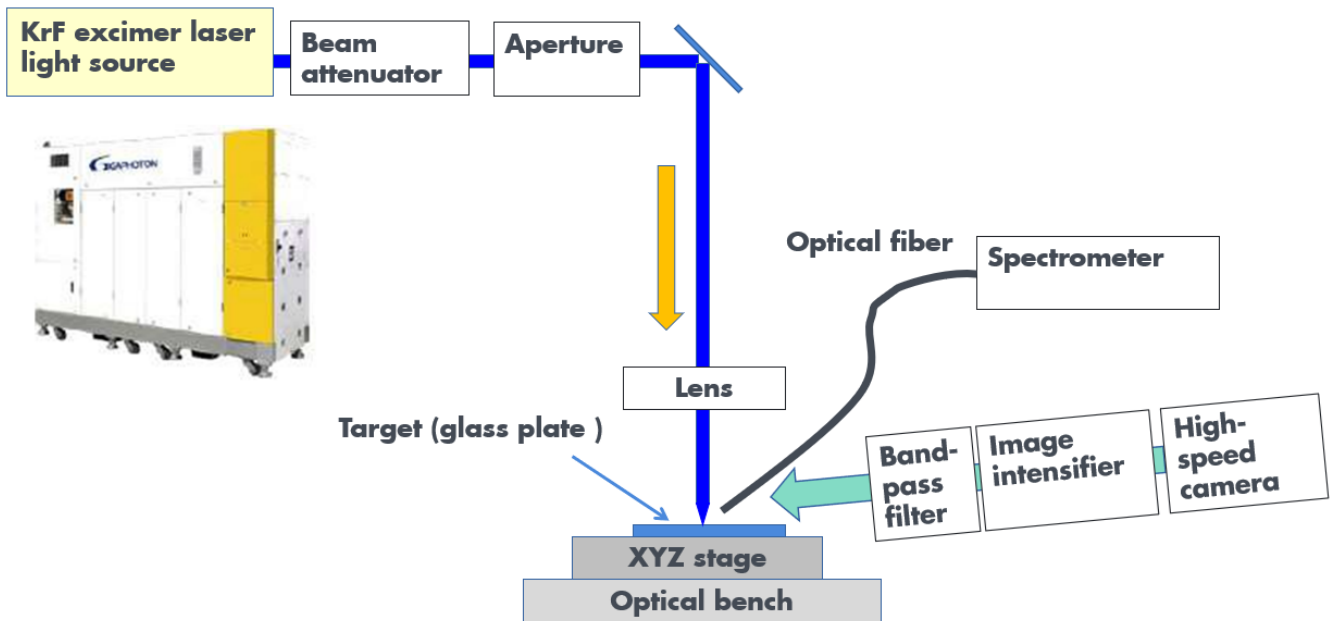


Fig. 1 Schematic diagram of laser processing test setup.

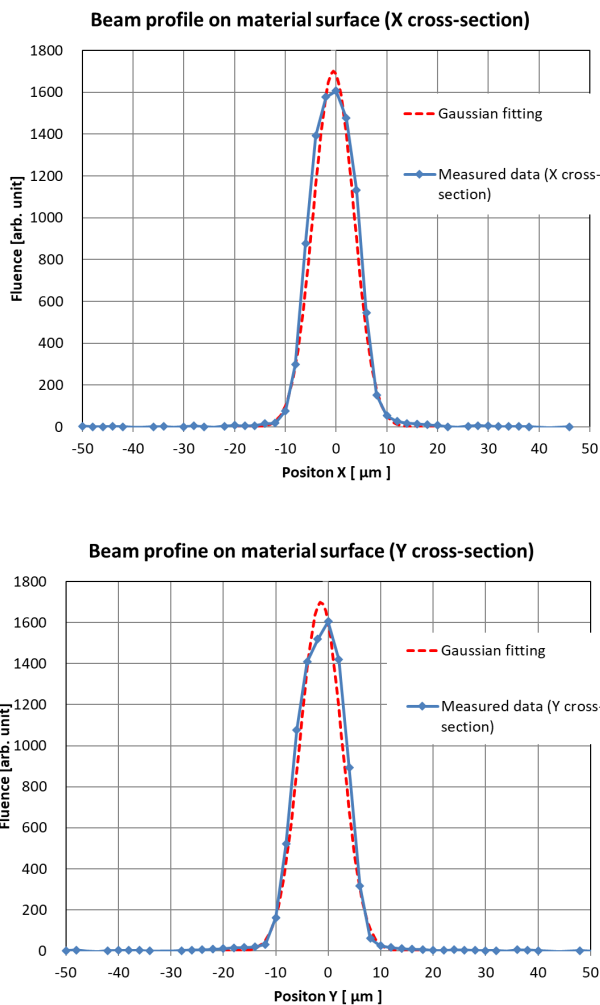
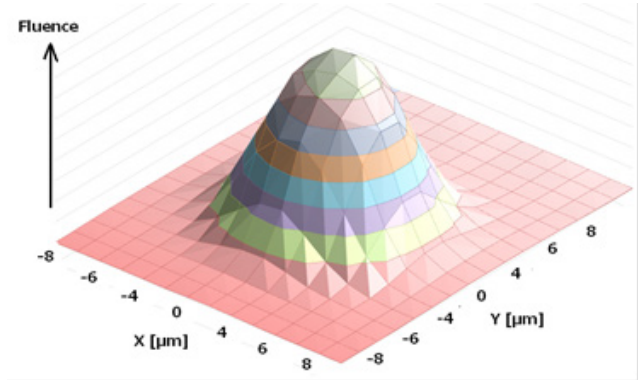
Table 3 Specifications of the test sample.

Material	Non-Alkali Glass
Type	Eagle XG
Thickness	500 μm
Supplier	Corning

Table 4 Instrumentation details.

Spectrometer	FLAME-S-UV-VIS (Ocean insight)
Image intensifier	UVi1850-10 (invisible vision)
High-speed camera	HX-5 (nac)
Bandpass filter	#35-881, #65-131, #34-497, #65-155 (Edmund)

The beam shape on the material surface is shown in Figures 2 (cross-sectional view) and 3 (isometric view). The beam shape was measured using an image sensor (OPHIR SP-928). The profile is Gaussian, and its diameter is $16.0\ \mu\text{m}$ ($1/e^2$), which is very close to the optical design target. The specifications of the test sample are given in Table 3. The measurement instrumentation details are given in Table 4.

**Fig. 2** Measured X and Y beam profiles on material surface (cross sectional view).**Fig. 3** Measured beam profile on material surface (isometric view).

3. Experimental result

3.1 Micro-via fabrication in glass

Micro-vias were successfully fabricated in glass by excimer laser ablation with no etching process required. The laser processing parameters are shown in table 5.

Peak fluence	36 [J/cm ²]
Spot Diameter	16 [μm] ($1/e^2$)
Laser frequency	100 [Hz]
Ambient condition	Atmosphere
Surface Gas flow of Glass	None

Table 5 Laser processing parameters used in the experiments.

Optical microscopy images of the resulting micro-vias in a 500-μm-thick glass substrate with a pitch of 30 μm are shown in Figures 4 (top view), 5 (side view), and 6 (bottom view).

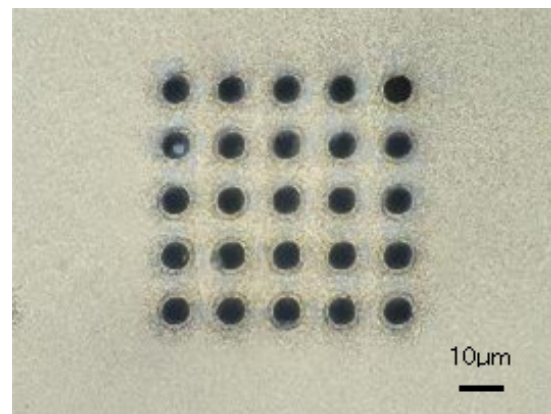
**Fig. 4** Top view of micro-vias fabricated in 500 μm thick glass.



Fig. 5 Side view of micro-vias fabricated by excimer laser ablation in 500 μm thick glass. Upper side is irradiation surface.

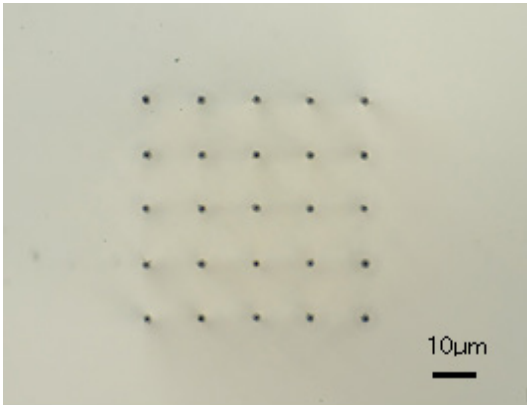


Fig. 6 Bottom view of micro-vias fabricated in 500 μm thick glass.

The diameter of the holes at the top surface is 15 μm , whereas that at the bottom surface is 2 μm . The aspect ratio of the micro-via holes is more than 33. Furthermore, no cracks were observed at the top or bottom surfaces, or inside the glass, despite being a brittle material.

3.1 Ablation rate measurement and pulse width dependence measurement of the glass material.

The ablation depth was measured from the side of the glass using an optical microscope (Olympus BX53M). Figures 7(a) and 7(b) show cross-sectional optical micrographs of vias formed using pulse width of 32 ns and 74 ns respectively. Figure 8 shows the dependence of the ablation

depth on the number of laser pulses with a central peak fluence of 36.0 J/cm² for a repetition rate of 100 Hz. These results show that the ablation rate increased with increasing laser pulse width.

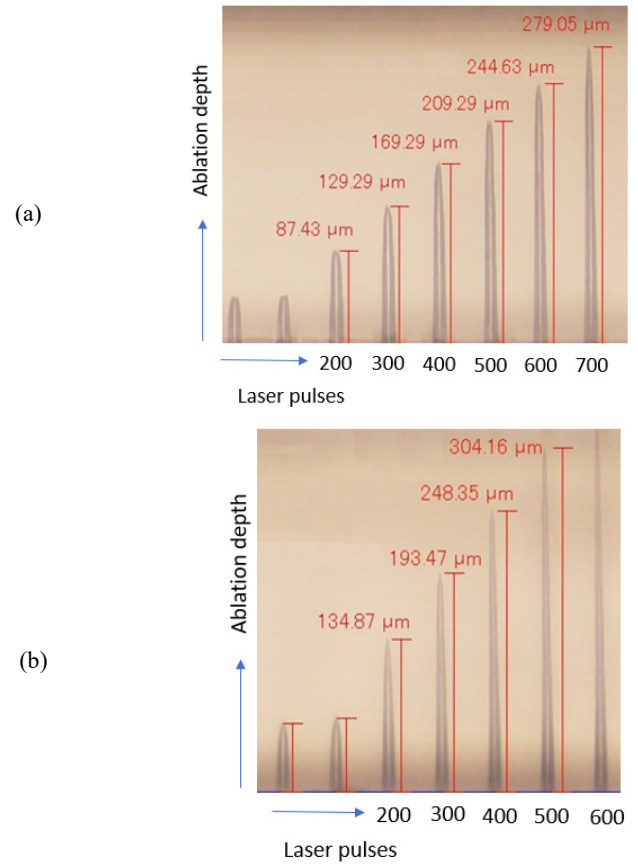


Fig. 7 Ablation depth measurement of every 100 pulses irradiation from the side of the glass by 32ns TIS laser pulse (a), 74ns TIS laser pulse (b) using a central peak fluence of 36.0J/cm² at 100Hz repetition rate. (Lower side is irradiation surface.)

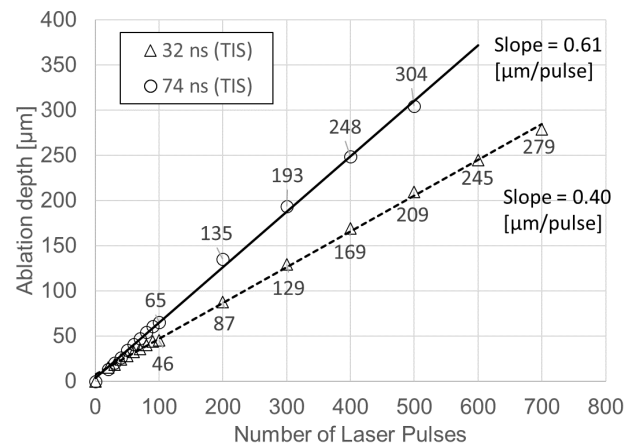


Fig. 8 Ablation depth and ablation rate for each irradiation pulse with ablation holes generated by 1 to 700 irradiation pulses using a central peak fluence of 39.0 J/cm² of 100Hz repetition rate with two different pulse widths.

3.2 Wavelength measurement of emission light with glass ablation

The optical spectrum of the light emitted during glass ablation was measured using a UV-vis spectrometer to investigate the ablation mechanism. Figure 9 shows a photograph of the emitted light, and Figure 10 shows the measured UV-vis spectrum. Table 6 lists the ions responsible for optical emission, and the main emission wavelengths. Aluminum atoms, which are a component of glass, are ionized during the ablation process.

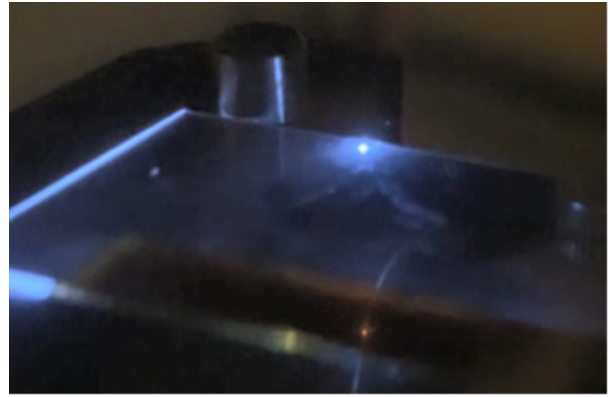


Fig. 9 Emission light during excimer laser ablation of glass.

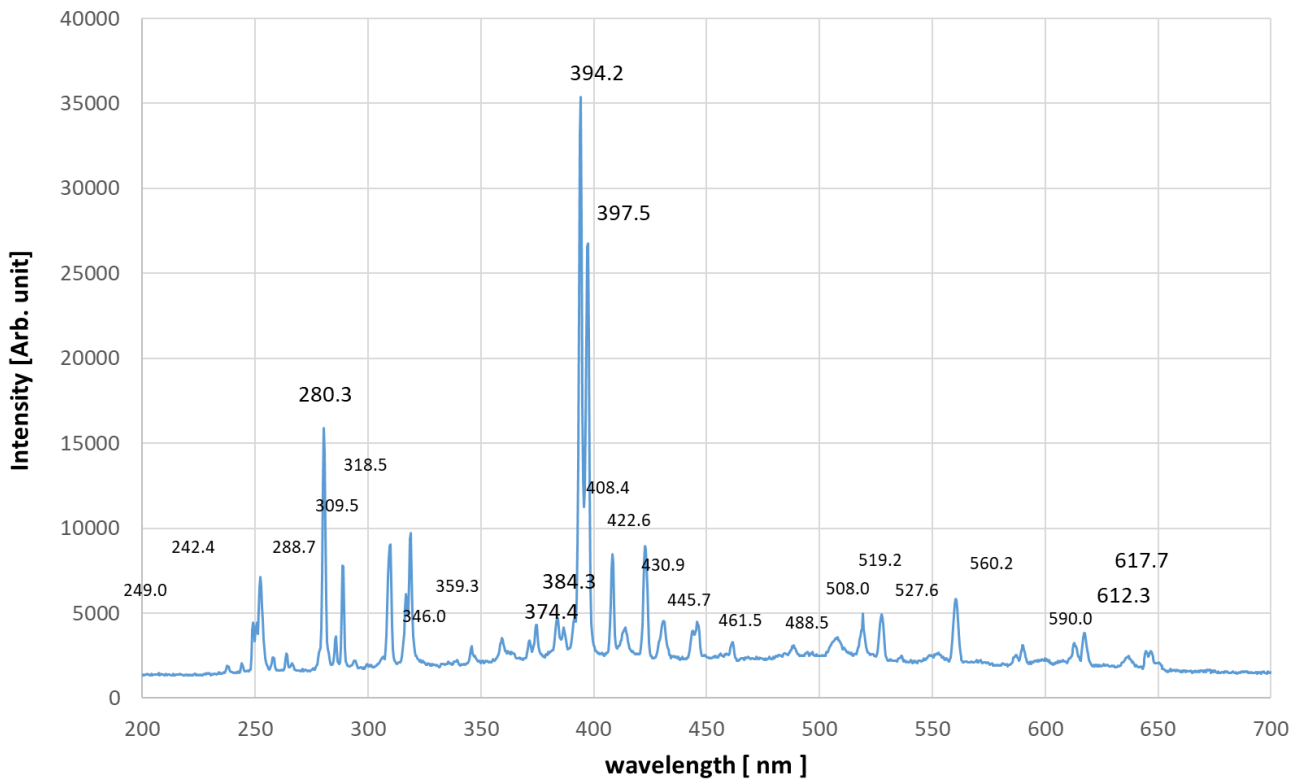


Fig. 10 Emission spectrum during excimer laser ablation of glass.

Table 6 Main emission wavelengths and ions produced during excimer laser ablation of glass.

Wavelength (nm)	Aluminum ion valence band
280 [nm]	2nd valence band
394 [nm]	1st valence band
422 [nm]	1st valence band
527 [nm]	2nd valence band

3.3 Time-resolved spectroscopy during glass ablation

Time-resolved spectroscopy was performed to investigate a mechanism for the higher ablation rate for longer pulses. The measurements were conducted using a band-pass filter (BPF), an image intensifier and a high-speed camera. Figure 11 shows the results as time-resolved band-pass images of ablation-induced optical emission using a 74-ns excimer laser. The exposure time for each image was 10 ns. The light intensity at each wavelength was measured as a function of time. Figure 12 shows the results for a 32-ns excimer laser. The waveforms for the 32-ns and 74-ns lasers are shown in Figure 13.

In Figure 10, the emission peak at 394 nm has the largest intensity. However, in Figures 11 and 12, the overall brightness at the end of BPF 394nm (about 300 ns) is smaller than that in the absence of BPF conditions. This is caused by the transmission of BPF of specified wavelength is about 60 %, and the absence of BPF image contains all wavelength (cf. 250 nm, 346 nm, 359 nm, etc.) intensity. The BPF that we used in this experiment optical specification is shown in Table 7.

In Figure 13, dips in the output intensity of the 74-ns laser can be observed at 25, 50 and 75 ns. These dips are generated by the OPS. We will evaluate the affect of this sag in future work.

Figure 14 shows the time dependence of the resolved emission line intensity for 72-ns and 32-ns pulses. For both pulse widths, emission begins approximately 30 ns after laser irradiation, which is considered to be the onset of ablation. This is thought to reflect the timescale for initial laser energy absorption by the glass. The mechanism of higher ablation rate for longer laser pulses is considered to be the larger amount of energy absorbed after ablation initially begins.

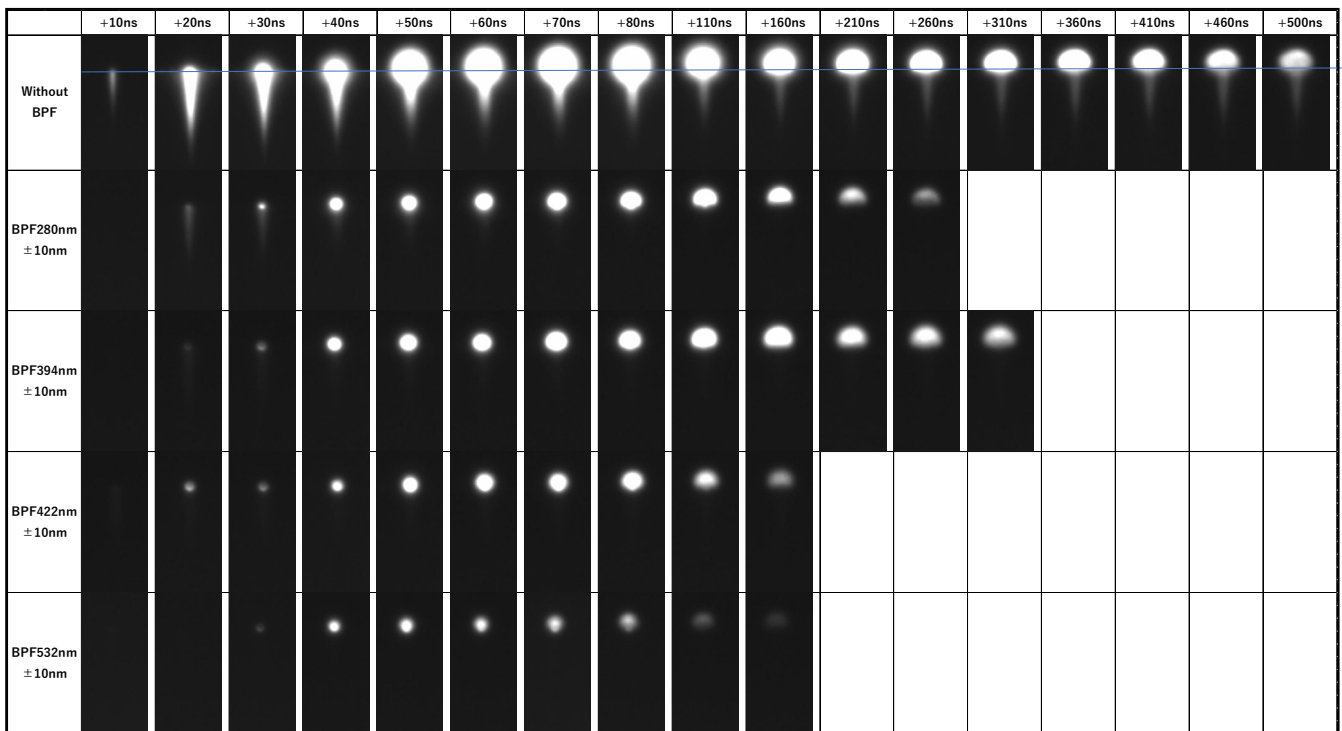
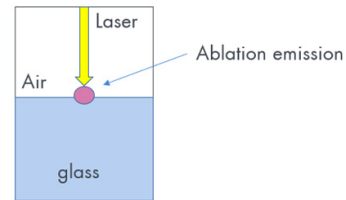
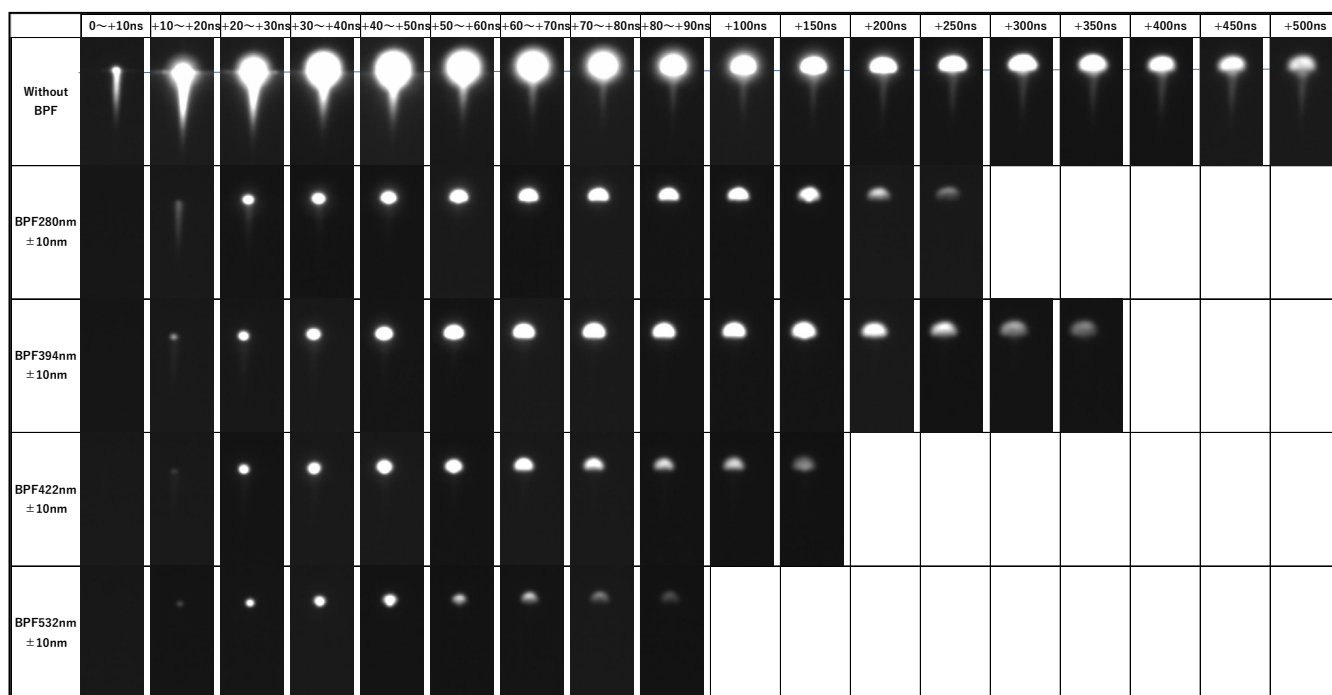
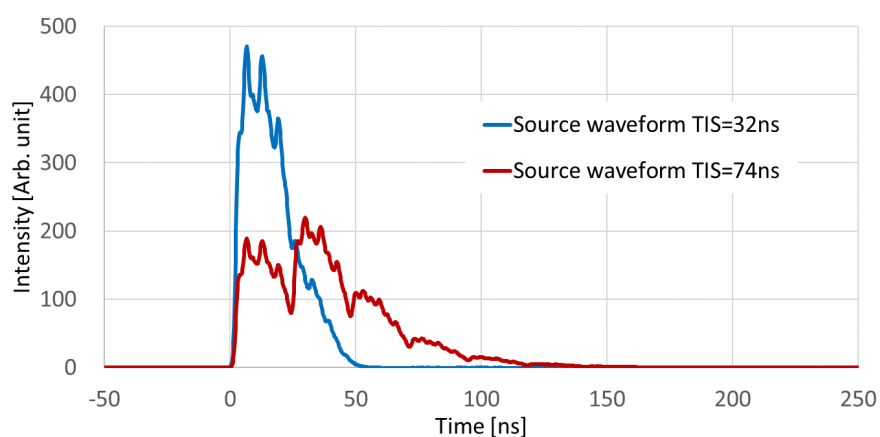


Fig. 11 Time-resolved bandpass image of ablation emission of glass of 74ns TIS excimer laser.

Table 7 Optical specification of BPF (Bandpass filter) .

Optical Density	>4.0
Transmission	>60 [%]
Passing Wavelength FWHM	10+/-2.0 [nm]
Blocking Wavelength range	200-650 [nm]

**Fig. 12** Time-resolved bandpass image of ablation emission of glass of 32ns TIS excimer laser.**Fig. 13** Pulse waveform of 32ns TIS and 74ns TIS of the laser light source.

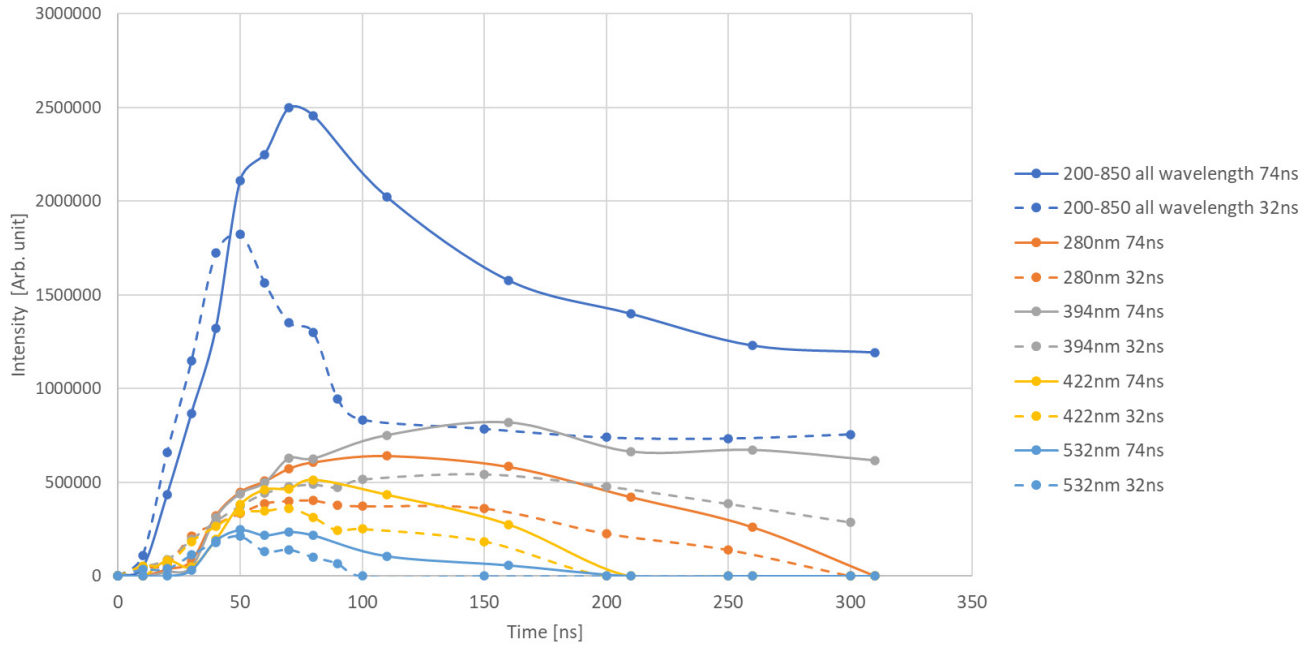


Fig. 14 Time dependence of resolved emission line intensity during glass ablation using long (solid lines) and short (dotted line) pulse widths.

4. Discussion

We found that the ablation rate for glass during micro-via formation using an excimer laser was higher for longer pulses. To determine the reason for this, we performed time-resolved spectroscopy during glass ablation using different laser pulse widths. The results indicated that ablation-induced optical emission begins 30 ns after laser irradiation. We conclude that the energy absorbed during this time period does not contribute to the glass drilling processing. Therefore, longer laser pulses contribute more energy to the actual ablation process. However, the reason for the delay of 30 ns is still unclear. At a wavelength of 248 nm, the transmittance of the glass used in the present study is 4300/m, which means that the absorbance within 1 μm from the surface is only 0.4%. It is presumed that the electron density in the surface region and the amount of heat absorbed increase during the initial period of 30 ns, until they reach the critical values required for ablation.

5. Conclusion

The fabrication of micro-vias in glass can be achieved by drilling using 248 nm excimer laser ablation with very high quality (15- μm diameter holes, no microcracks), high aspect ratio (>30), and high productivity due to the high power of the excimer laser (>300 W). The ablation rate can be improved by increasing the laser pulse width using an OPS. The rate was improved by 50% when the pulse width was 74 ns, compared with that using 32-ns pulses. The light emitted during ablation was spectroscopically analyzed and was found to be mainly due to aluminum ions. Emission began 30 ns after laser irradiation, regardless of the laser pulse width. The higher ablation rate for longer

pulses is thought to be due to the larger amount of energy deposited after the critical ablation threshold is reached. In future studies, we plan to further increase the laser pulse width and investigate its effect on the ablation rate. The present study established the feasibility of fabricating high-quality micro-vias in glass interposer substrates for 5G and post-5G glass applications.

Acknowledgement

This paper is based on results obtained from a project, JPNP20017, subsidized by the New Energy and Industrial Technology Development Organization (NEDO) Japan.

References

- [1] J. Ihlemann and B. Wolff-Rottke: Appl. Surf. Sci., 106, (1996) 282
- [2] R. Karstens, A. Gödecke, A. Prießner, and J. Ihlemann: Opt. Laser Technol., 83, (2016) 16
- [3] J. Ihlemann, B. Wolff and P. Simon, Appl. Phys. A, 54, (1992) 263
- [4] Yasufumi Kawasuji, Junichi Fujimoto, Masakazu Kobayashi, Akira Suwa, Akira Mizutani, Masaki Arakawa, Takashi Onose, and Hakaru Mizoguchi: J. Laser Appl., 32, (2020) 022076

(Received: April 13, 2022, Accepted: October 15, 2022)